Optical CDMA with Embedded Spectral-Polarization Coding over Double Balanced Differential-Detector

Jen-Fa Huang, Chih-Ta Yen, and Bo-Hau Chen

Institute of Computer and Communications, Department of Electrical Engineering,
National Cheng Kung University, Tainan City, Taiwan, ROC
huajf@ee.ncku.edu.tw

Abstract. A spectral-polarization coding (SPC) optical code-division multiple-access (OCDMA) configuration structured over arrayed-waveguide grating (AWG) router is proposed. The polarization-division double balanced detector is adopted to execute difference detection and enhances system performance. The signal-to-noise ratio (SNR) is derived by taking the effect of PIIN into account. The result indicates that there would be up to 9-dB SNR improvement than the conventional spectral-amplitude coding (SAC) structures with Walsh-Hadamard codes. Mathematical deriving results of the SNR demonstrate the system embedded with the orthogonal state of polarization (SOP) will suppress effectively phase-induced intensity noise (PIIN). In addition, we will analyze the relations about bit error rate (BER) vs. the number of active users under the different encoding schemes and compare them with our proposed scheme. The BER vs. the effective power under the different encoding scheme with the same number of simultaneous active user conditions are also revealed. Finally, the polarization-matched factor and the difference between simulated and experimental values are discussed.

Keywords: spectral polarization coding, optical code-division multiple-access, arrayed-waveguide grating, polarization-division double balanced differential-detector, phase-induced intensity noise, Walsh-Hadamard codes.

1 Introduction

The optical code-division multiple-access (OCDMA) technique in optical communication is gradually noticed in the recent years for requirement of multiple users can access the network asynchronously and simultaneously with high level transmission security [1-3]. The spectral-amplitude coding optical code-division multiple-access (SAC-OCDMA) system was proposed as a means of increasing the maximum permissible number of simultaneous active users by decreasing the codeword length and eliminating the multiple-access interference (MAI) effect [4]-[7]. With regard to spectral-amplitude coding (SAC) technique, it is crucial to identify the maximum number of wavelengths that such dispersive devices could resolve, since this will dictate the length of the code employed for coding. The SAC-OCDMA system not only preserves the ability of MAI cancellation, but also uses cheap sources with reduced complexity. However, in the traditional SAC scheme, the effect of

C. Wang (Ed.): AccessNets, LNICST 6, pp. 441–456, 2009.

polarization is often ignored in the procedure of encoding and decoding. While photodiodes (PDs) are applied to detect in the receiver, the phase-induced intensity noise (PIIN) cannot be suppressed and the signal-to-noise ratio (SNR) of system is degraded. Smith et al. [8] have concluded that the performance of SAC schemes is limited by the presence of beat noise. Hence, the performance is hard to boost enormously even though using the bipolar scheme [9].

A fundamental approach to the PIIN problem is to reduce the number of wavelength collisions in the balanced photo-detector. In the spectral-polarization coding (SPC) scheme proposed in the current study [10], a Walsh-Hadamard code is employed as signature address accomplishing by fiber Bragg gratings (FBGs). This code is characterized by a bipolar property [11] due to orthogonality among states of polarization (SOPs). The spectral efficiency of the proposed complementary bipolar scheme is found to be twice that of the previous unipolar supercodes. Thus, the proposed SPC approach enables a dramatic increase in the permissible number of simultaneous active users for the same optical bandwidth. The other advantage of the proposed system is that the use of two orthogonally polarized chips transmitted at the same wavelength from the same encoder eliminates PIIN.

Since a single-mode fiber (SMF) supports two orthogonal SOPs for the same fundamental mode, a new kind of multiplexing, known as the Polarization-division multiplexing (PDM), in which two orthogonally polarized signals are transmitted simultaneously in a, provides a versatile solution for increasing the utilization of the available bandwidth. In PDM, two channels at the same wavelength are transmitted through the fiber such that their pulse trains are orthogonally polarized at the fiber input. At first glance, such a scheme should not work unless polarization-maintaining fibers (PMFs) are used since the polarization state changes randomly in conventional fibers because of birefringence fluctuations. However, even though the polarization states of each channel does change at the end of the fiber link in an unpredictable manner, their orthogonal nature is preserved, making it possible to isolate each channel through simple optical techniques. Various combinations of PDM with other multiplexing techniques have been proposed [12]-[14]. In [14], the respect to polarization, an arrayed-waveguide grating (AWG) is a linear device, and thus the degree of polarization (DOP) of the AWG-based system should not degrade. Besides, multi-wave optical sources could be used in the PDM transmission systems [15]. However, the PDM demultiplexing technique is rather complex due to the random change of the signal's SOP caused by fluctuations of the fiber birefringence along the fiber's length. This phenomenon induces so-called polarization mode dispersion (PMD). It means that there are two orthogonal polarization modes, which are called principal states of polarization (PSPs) [16], obeying different dispersion relations. Recently, PMD compensation techniques have been applied successfully to enhance the performance of WDM systems as in [17] and [18]. In the general PMD compensation approach, a feedback signal is employed to tune the adaptive polarization controller [19] and delay line [20] in order to adjust the PSPs and the differential group delay (DGD). Such advanced PMD compensation techniques render the proposed SPC scheme feasible for implementation in long-haul networks [21].

The remainder of this paper is organized as follows. Section 2 introduces the proposed system configuration and explains the encoder/decoder (codec) mechanisms. Section 3 describes the encoding/decoding schemes and illustrates the elimination of

MAI by mathematical analyses. Section 4 derives the SNR of the proposed structure and evaluates the system performance in terms of the bit error rate (BER) and the maximum number of permissible simultaneous active users. The analytic results are compared with those of the conventional unipolar and bipolar SAC schemes approach to evaluate the performance improvement. Section 5 compares and discusses some related-curve diagrams of the BER versus effective power under the different number of active users and the different coding schemes with our proposed scheme. Finally, Section 6 provides some concluding remarks.

2 System Configuration

2.1 Encoder Scheme

The OCDMA network coder embedded SPC and polarization-division double balanced differential-detection technique is constructed on the basis of AWGs as shown in Fig. 1. Due to transmitted information data bit for each user is different, the optical polarization modulated module shown at left side in Fig. 1 is independent. In addition, the polarization-division double balanced detector shown at right side in Fig. 1 is also one by one for each user. The encoding procedure includes four steps.

1. A broadband optical source is adopting the modulating source. Then passing through a splitter, it is modulated by desired data and its counterpart, $\overline{\text{data}}$, respectively.
2. The modulated optical sources are introduced PBSs to divide mutually orthogonal SOPs. After electric-optical modulator (EOM), a polarization controller (PC) is set to adjust the SOP between an EOM and a PBS. Then two mutually orthogonal SOP optical elements input to the AWG-based OCDMA encoder.
3. According to the wavelength cyclic shifted property of AWGs, two orthogonal SOPs are inputted different input ports of AWG to obtain a set of Walsh-Hadamard code and its complementary code that accompany the mutually orthogonal SOPs. Namely, there will be the spectrum of $\boldsymbol{C}_j$ (H) and $\overline{\boldsymbol{C}}_j$ (V) at the upper branch. Note that the sub-index means the codeword is used for user #$\boldsymbol{j}$; (H) and (V) denote the horizontal and vertical SOP, respectively. Similarly, $\boldsymbol{C}_j$ (V) and $\overline{\boldsymbol{C}}_1$ (H) output at the lower branch.
4. Finally, the encoded spectrum for user #$\boldsymbol{j}$ is accomplished by combining two branches.

2.2 Decoder Scheme

The decoding processes can be divided into three steps and explain as following.

1. Taking out the mutually orthogonal SOP components from the encoded spectrum, then input to AWG router to perform OCDMA decoding process.
2. Depend on decoded signature code $\boldsymbol{C}_j$ and its complementary, $\overline{\boldsymbol{C}}_j$ to determine which output port of AWG routers should be coupled each other of star couplers.

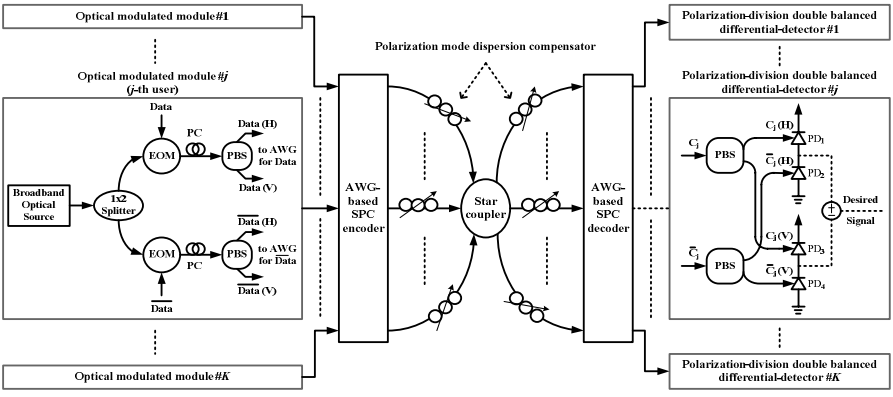

Fig. 1. System structure of proposed SPC scheme with polarization-division double balanced differential-detector

3. The spectra have the same SOP are executed to realize balanced detection, i.e., the detected electrical signals form the lower branch is subtracted from the correspondence from the upper branch. Finally, the desired data signal for user ***#j*** can be obtained.

3 Mathematical Analyses

3.1 Codec Scheme over AWG-Based

In Fig. 1, if we consider that K transmitter/receiver pairs are connected to a passive $2K$x1 star coupler. Meanwhile, a set of Walsh-Hadamard code is denoted by $\boldsymbol{C}_k$ and its complementary code $\overline{\boldsymbol{C}}_k$, is assigned to the k-th user. Here we give an example for the number of user equals 7, i.e. $K = 7$, as shown in Fig. 2. The index i of $\mathrm{H}_i/\mathrm{V}_i$ denotes horizontal/vertical quantity of the i-th user.

By adopting the wavelength cyclic shifted property of AWG routers, we can get the spectra are $\boldsymbol{C}_k(\mathrm{H}) + \overline{\boldsymbol{C}}_k(\mathrm{V})$ and $\boldsymbol{C}_k(\mathrm{V}) + \overline{\boldsymbol{C}}_k(\mathrm{H})$ at the output of the 4x1 star coupler in the upper and the lower branch, respectively. Therefore, the horizontal and vertical quantity spectra are written as

$$\boldsymbol{E}_{\mathrm{H}} = \sum_{k=1}^{K} b_k \boldsymbol{C}_k + \bar{b}_k \overline{\boldsymbol{C}}_k \ , \tag{1a}$$

$$\boldsymbol{E}_{\mathrm{V}} = \sum_{k=1}^{K} b_k \overline{\boldsymbol{C}}_k + \bar{b}_k \boldsymbol{C}_k \ , \tag{1b}$$

where b_k is the k-th user's data bit ($b_k \in \{0,1\}$), and $\boldsymbol{C}_k$ and $\overline{\boldsymbol{C}}_{\mathrm{k}}$ are respectively the k-th user's direct and complementary codewords in the spectral domain. The summed

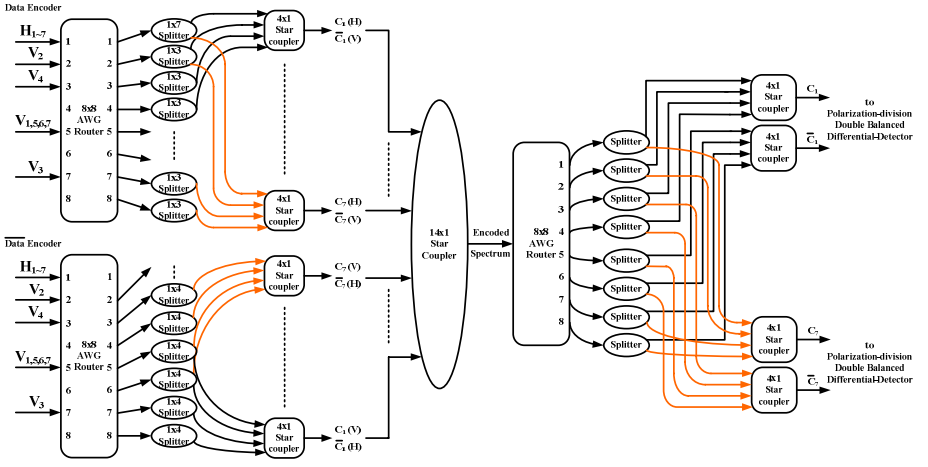

Fig. 2. Structure diagram of AWG-based SPC codec in detail

signal spectrum for all the simultaneous active user, $\boldsymbol{R}$, is composed of horizontal and vertical states of polarization and is given by

$$\boldsymbol{R} = \boldsymbol{E}_{\mathrm{H}} + \boldsymbol{E}_{\mathrm{V}} . \tag{2}$$

Then the encoded spectrum is sent to the decoder as shown in Fig. 2. After the decoding procedure as described in subsection 2.2 at Section 2, we can obtain the corresponding spectrum for each user's upper branch and lower branch at output of star couplers in the decoder. They are expressed in Eqs. (3a) and (3b), respectively,

$$\boldsymbol{R} \cdot \boldsymbol{C}_k = \sum_{k=1}^{K} b_k \boldsymbol{C}_k + \bar{b}_k \boldsymbol{C}_k . \tag{3a}$$

$$\boldsymbol{R} \cdot \overline{\boldsymbol{C}}_k = \sum_{k=1}^{K} \bar{b}_k \overline{\boldsymbol{C}}_k + b_k \overline{\boldsymbol{C}}_k . \tag{3b}$$

In Eqs. (3a) and (3b), the first item belongs to horizontal SOP quantity and the last item belongs to vertical SOP quantity. Moreover, according to the proposed structure, we take out horizontal and vertical components from above two equations to execute the double balanced detection. It is expressed as

$$\sum_{k=1}^{K} [b_k (\boldsymbol{C}_k + \overline{\boldsymbol{C}}_k) - \bar{b}_k (\boldsymbol{C}_k + \overline{\boldsymbol{C}}_k)]$$

$$= \begin{cases} \sum_{k=1}^{K} (\boldsymbol{C}_k + \overline{\boldsymbol{C}}_k) = N & \text{for } b_k = 1 , \\ -\sum_{k=1}^{K} (\boldsymbol{C}_k + \overline{\boldsymbol{C}}_k) = -N & \text{for } b_k = 0 \end{cases} \tag{4}$$

where N is indicated the codeword length.

3.2 MAI Cancellation

The encoded spectrum can be obtained in (2). From (3a), by replacing the external $\boldsymbol{C}_k$ becomes to $\boldsymbol{C}_j$, the equation is rewritten as

$$\boldsymbol{R}\cdot\boldsymbol{C}_j=[\sum_{k=1}^{K}(b_k\boldsymbol{C}_k+\bar{b}_k\overline{\boldsymbol{C}}_k)+\sum_{k=1}^{K}(b_k\overline{\boldsymbol{C}}_k+\bar{b}_k\boldsymbol{C}_k)]\cdot\boldsymbol{C}_j. \tag{5a}$$

Similarly, we update (3b) as shown below.

$$\boldsymbol{R}\cdot\overline{\boldsymbol{C}}_j=[\sum_{k=1}^{K}(b_k\boldsymbol{C}_k+\bar{b}_k\overline{\boldsymbol{C}}_k)+\sum_{k=1}^{K}(b_k\overline{\boldsymbol{C}}_k+\bar{b}_k\boldsymbol{C}_k)]\cdot\overline{\boldsymbol{C}}_j. \tag{5b}$$

In the above equations, the former items in the middle brackets are still represented the horizontal SOP quantity. The latter items are the vertical SOP quantity. According to our polarization-division decoding scheme, we make the parts have the same SOP to execute balanced detection.

$$(5a)_{(H)}-(5b)_{(H)}\Rightarrow$$
$$\sum_{k=1}^{K}[b_k(\boldsymbol{C}_k\cdot\boldsymbol{C}_j-\boldsymbol{C}_k\cdot\overline{\boldsymbol{C}}_j)+\bar{b}_k(\overline{\boldsymbol{C}}_k\cdot\boldsymbol{C}_j-\overline{\boldsymbol{C}}_k\cdot\overline{\boldsymbol{C}}_j)]. \tag{6a}$$

$$(5a)_{(V)}-(5b)_{(V)}\Rightarrow$$
$$\sum_{k=1}^{K}[b_k(\overline{\boldsymbol{C}}_k\cdot\boldsymbol{C}_j-\overline{\boldsymbol{C}}_k\cdot\overline{\boldsymbol{C}}_j)+\bar{b}_k(\boldsymbol{C}_k\cdot\boldsymbol{C}_j-\boldsymbol{C}_k\cdot\overline{\boldsymbol{C}}_j)]. \tag{6b}$$

By introducing the following Walsh-Hadamard codes correlation properties into Eqs. (6a) and (6b),

$$R_{\boldsymbol{cc}}(k,l)=\sum_{i=1}^{N}\boldsymbol{C}_k(i)\boldsymbol{C}_l(i)=\begin{cases}N/2\ , & \text{for } k=l\\ N/4\ , & \text{for } k\neq l\end{cases}, \tag{7a}$$

and

$$R_{\boldsymbol{c}\bar{\boldsymbol{c}}}(k,l)=\sum_{i=1}^{N}\boldsymbol{C}_k(i)\overline{\boldsymbol{C}}_l(i)=\begin{cases}0\ , & \text{for } k=l\\ N/4\ , & \text{for } k\neq l\end{cases}. \tag{7b}$$

We will get an answer of zero when the decoded pattern does not match the coded pattern. Namely, the MAI is eliminated completely in theory for the idea flat spectrum of an incoherent optical source.

Table 1 presents an example of the SPC with polarization-division double balanced differential-detection mechanism for simultaneous active users $K = 3$ and code length $N = 8$. In the illustration, users #1 and #2 transmit logical 1 information bit, and user #3 sends logical 0. We assume the optical source has the ideal flat spectrum and the power unit of each wavelength is equal. Applying our proposed encoding process, the resultant code vectors are $\boldsymbol{E}_{\mathrm{H}}$ = ($2\lambda_1$, $2\lambda_2$, $3\lambda_3$, $1\lambda_4$, $1\lambda_5$, $1\lambda_6$, $2\lambda_7$, $0\lambda_8$) and $\boldsymbol{E}_{\mathrm{V}}$ = ($1\lambda_1$, $1\lambda_2$, $0\lambda_3$, $2\lambda_4$, $2\lambda_5$, $2\lambda_6$, $1\lambda_7$, $3\lambda_8$). When the received signal $\boldsymbol{R}$ pass through the decoder #1, 8 units photocurrent are yielded, which corresponds signature code word, $\boldsymbol{C}_1$, and

horizontal SOP at PD_1 as shown in Fig. 1. In the same method, 4 units photocurrent are obtained for $\overline{\boldsymbol{C}}_1$ with horizontal SOP at PD_2. Moreover, the 4 units and 8 units photocurrent are matched $\boldsymbol{C}_1$ (V) and $\overline{\boldsymbol{C}}_1$ (V) at PD_3 and PD_4 in the lower arm, respectively. And the numerical values could be calculated by (5a) and (5b). Balanced differential-detection results in $\boldsymbol{R}\boldsymbol{C}_1^{(\mathrm{H})} - \boldsymbol{R}\overline{\boldsymbol{C}}_1^{(\mathrm{H})} = 4$ units power and $\boldsymbol{R}\boldsymbol{C}_1^{(\mathrm{V})} - \boldsymbol{R}\overline{\boldsymbol{C}}_1^{(\mathrm{V})} = -4$ units power. After the second stage differential detecting, 8 units power is obtained and decides that logic "1" is transmitted. Similarly, if substituting decoder #3 for #1, 4, 8, 8, 4 units power photocurrent would be detected at PD_1, PD_2, PD_3, and PD_4, respectively.

Table 1. Simple illustration of polarization-division balanced differential-detection for 3 simultaneous active users

Spectral Polarization Coding Mechanism																		
User	**Data bit**	**Horizontal SOP**									**Vertical SOP**								
			λ_1	λ_2	λ_3	λ_4	λ_5	λ_6	λ_7	λ_8		λ_1	λ_2	λ_3	λ_4	λ_5	λ_6	λ_7	λ_8
1	1	$\boldsymbol{C}_1$	1	1	1	1	0	0	0	0	$\overline{\boldsymbol{C}}_1$	0	0	0	0	1	1	1	1
2	1	$\boldsymbol{C}_2$	1	0	1	0	1	0	1	0	$\overline{\boldsymbol{C}}_2$	0	1	0	1	0	1	0	1
3	0	$\overline{\boldsymbol{C}}_3$	0	1	1	0	0	1	1	0	$\boldsymbol{C}_3$	1	0	0	1	1	0	0	1
Received Signal ($\boldsymbol{R}$)		$\boldsymbol{E}_{\mathrm{H}}$	2	2	3	1	1	1	2	0	$\boldsymbol{E}_{\mathrm{V}}$	1	1	0	2	2	2	1	3

Finally, -8 units power will occur in decoder #3 and indicates user #3 sent logic "0". In the decoders of other users, e.g., $\boldsymbol{C}_4$ = (1, 1, 0, 0, 0, 0, 1, 1), the unit power at each PD is equal. After double balanced differential-detection, it will no power is detected. Hence, MAI from other users with differential detection scheme can be theoretically cancelled.

4 Performance Analysis

4.1 Signal Power Evaluation

Referring to [3] and [10], and applying (2), the detected photo-current coming from K simultaneous active users with a chip length N per user, $\boldsymbol{I}_1$, from PD_1 shown in Fig. 9, is written as

$$\begin{aligned} \boldsymbol{I}_1 &= \Re \int_0^\infty G_1(\nu) d\nu \\ &= \frac{\Re P_{sr}}{\sqrt{2}N} \sum_{i=1}^{N} \sum_{k=1}^{K} \{ b_k [\boldsymbol{C}_k(i) \cdot \boldsymbol{C}_j(i)] + \bar{b}_k [\overline{\boldsymbol{C}}_k(i) \cdot \boldsymbol{C}_j(i)] \} \end{aligned}, \tag{8a}$$

where $\Re$ denotes the responsibility of the PD, $G_1(\nu)$ is the single-sideband power spectral densities (PSDs) of the received signal at PD_1, and P_{sr} is the effective power from a single source at the receiver. The coefficient $\sqrt{2}$ is as a result of adopting PBS. Similarly, the detected photocurrents at photodiode PD_2, PD_3, and PD_4 are written as $\boldsymbol{I}_2$, $\boldsymbol{I}_3$, $\boldsymbol{I}_4$, respectively.

$$\begin{aligned}\boldsymbol{I}_2 &= \Re\int_0^\infty G_2(\nu)\,d\nu \\ &= \frac{\Re P_{sr}}{\sqrt{2}N}\sum_{i=1}^{N}\sum_{k=1}^{K}\{b_k[\boldsymbol{C}_k(i)\cdot\overline{\boldsymbol{C}}_j(i)]+\overline{b}_k[\overline{\boldsymbol{C}}_k(i)\cdot\overline{\boldsymbol{C}}_j(i)]\}\end{aligned}. \tag{8b}$$

$$\begin{aligned}\boldsymbol{I}_3 &= \Re\int_0^\infty G_3(\nu)\,d\nu \\ &= \frac{\Re P_{sr}}{\sqrt{2}N}\sum_{i=1}^{N}\sum_{k=1}^{K}\{b_k[\overline{\boldsymbol{C}}_k(i)\cdot\boldsymbol{C}_j(i)]+\overline{b}_k[\boldsymbol{C}_k(i)\cdot\boldsymbol{C}_j(i)]\}\end{aligned}. \tag{8c}$$

$$\begin{aligned}\boldsymbol{I}_4 &= \Re\int_0^\infty G_4(\nu)\,d\nu \\ &= \frac{\Re P_{sr}}{\sqrt{2}N}\sum_{i=1}^{N}\sum_{k=1}^{K}\{b_k[\overline{\boldsymbol{C}}_k(i)\cdot\overline{\boldsymbol{C}}_j(i)]+\overline{b}_k[\boldsymbol{C}_k(i)\cdot\overline{\boldsymbol{C}}_j(i)]\}\end{aligned}. \tag{8d}$$

The signal from the desired user is given by the difference of the photocurrent outputs. After the second stage balanced detection is expressed as

$$\begin{aligned}\boldsymbol{I} &= (\boldsymbol{I}_1-\boldsymbol{I}_2)-(\boldsymbol{I}_3-\boldsymbol{I}_4) \\ &= \frac{\Re P_{sr}}{\sqrt{2}N}\sum_{i=1}^{N}\sum_{k=1}^{K}\{b_k[\boldsymbol{C}_k(i)\cdot\boldsymbol{C}_j(i)-\boldsymbol{C}_k(i)\cdot\overline{\boldsymbol{C}}_j(i) \\ &\qquad -\overline{\boldsymbol{C}}_k(i)\cdot\boldsymbol{C}_j(i)+\overline{\boldsymbol{C}}_k(i)\cdot\overline{\boldsymbol{C}}_j(i)] \\ &\qquad +\overline{b}_k[\overline{\boldsymbol{C}}_k(i)\cdot\boldsymbol{C}_j(i)-\overline{\boldsymbol{C}}_k(i)\cdot\overline{\boldsymbol{C}}_j(i) \\ &\qquad -\boldsymbol{C}_k(i)\cdot\boldsymbol{C}_j(i)+\boldsymbol{C}_k(i)\cdot\overline{\boldsymbol{C}}_j(i)]\}\end{aligned}. \tag{9}$$

By introducing the correlation properties of Eqs. (7a) and (7b), Equ. (9) can be simplified to be

$$\boldsymbol{I} = \begin{cases} \Re P_{sr}/\sqrt{2} & \text{for } k=j \text{ and } b_k=1 \\ -\Re P_{sr}/\sqrt{2} & \text{for } k=j \text{ and } b_k=0 \\ 0 & \text{for } k\neq j \end{cases}. \tag{10}$$

4.2 PIIN Power Evaluation

Noise that exists in the SAC-OCDMA systems includes PIIN, shot noise and thermal noise. The mathematical description is given by

$$\begin{aligned}\left\langle i^2\right\rangle &= \left\langle \boldsymbol{I}_{\text{shot}}^2\right\rangle + \left\langle \boldsymbol{I}_{\text{PIIN}}^2\right\rangle + \left\langle \boldsymbol{I}_{\text{thermal}}^2\right\rangle \\ &= 2e\boldsymbol{I}B + \boldsymbol{I}^2 B\tau_c + 4K_bT_nB/R_L\end{aligned}, \tag{11}$$

where e is the electron's charge, $\boldsymbol{I}$ is the average photocurrent, B is the noise-equivalent electrical bandwidth of the receiver, τ_c is the coherence time of the source, K_b is the Boltzmann's constant, T_n is the absolute receiver noise temperature, and R_L is the receiver load resistor. PIIN is the dominating noise when the received optical power is large enough (more than -10 dBm), we ignore the effect of other noises in large received effective power condition. So, the variance of photocurrent due to the effect of PIIN can be written as

$$\left\langle i^2 \right\rangle \cong \left\langle \boldsymbol{I}_{\mathrm{PIIN}}^2 \right\rangle = \boldsymbol{I}^2 (1+P^2) B\tau_c \,, \tag{12}$$

where P denotes the DOP. Base on the proposed scheme, the parameter P is set to 1. Hence, (12) can be rewritten as

$$\begin{aligned} \left\langle \boldsymbol{I}_{\mathrm{PIIN}}^2 \right\rangle &= 2\boldsymbol{I}^2 B\tau_c \\ &= 2B\Re^2 \sum_{m=1}^{4} \left(\int_0^\infty G_m^2(\nu)\, d\nu\right) \end{aligned}, \tag{13}$$

where m is the number of PD are used in our proposing structure. The light source spectrum is assumed to be idea flat with linewidth, $\Delta\nu$. The variance of the photocurrent resulting from the PIIN at PD_1 is expressed as

$$\begin{aligned} \left\langle \boldsymbol{I}_1^2 \right\rangle = \frac{B\Re^2 P_{sr}^2}{2N\Delta\nu} \sum_{i=1}^{N} \sum_{k=1}^{K} \sum_{m=1}^{K} [&b_k b_m \boldsymbol{C}_k(i)\boldsymbol{C}_m(i)\boldsymbol{C}_j(i) \\ &+ b_k \bar{b}_m \boldsymbol{C}_k(i)\overline{\boldsymbol{C}}_m(i)\boldsymbol{C}_j(i) \\ &+ \bar{b}_k b_m \overline{\boldsymbol{C}}_k(i)\boldsymbol{C}_m(i)\boldsymbol{C}_j(i) \\ &+ \bar{b}_k \bar{b}_m \overline{\boldsymbol{C}}_k(i)\overline{\boldsymbol{C}}_m(i)\boldsymbol{C}_j(i)] \end{aligned} \,. \tag{14a}$$

In the same way, the variances of the photocurrent are generated by the others PDs (i.e. PD_2, PD_3, and PD_4) can be written as (14b), (14c), and (14d), respectively.

$$\begin{aligned} \left\langle \boldsymbol{I}_2^2 \right\rangle = \frac{B\Re^2 P_{sr}^2}{2N\Delta\nu} \sum_{i=1}^{N} \sum_{k=1}^{K} \sum_{m=1}^{K} [&b_k b_m \boldsymbol{C}_k(i)\boldsymbol{C}_m(i)\overline{\boldsymbol{C}}_j(i) \\ &+ b_k \bar{b}_m \boldsymbol{C}_k(i)\overline{\boldsymbol{C}}_m(i)\overline{\boldsymbol{C}}_j(i) \\ &+ \bar{b}_k b_m \overline{\boldsymbol{C}}_k(i)\boldsymbol{C}_m(i)\overline{\boldsymbol{C}}_j(i) \\ &+ \bar{b}_k \bar{b}_m \overline{\boldsymbol{C}}_k(i)\overline{\boldsymbol{C}}_m(i)\overline{\boldsymbol{C}}_j(i)] \end{aligned} \,. \tag{14b}$$

$$\begin{aligned} \left\langle \boldsymbol{I}_3^2 \right\rangle = \frac{B\Re^2 P_{sr}^2}{2N\Delta\nu} \sum_{i=1}^{N} \sum_{k=1}^{K} \sum_{m=1}^{K} [&b_k b_m \overline{\boldsymbol{C}}_k(i)\overline{\boldsymbol{C}}_m(i)\boldsymbol{C}_j(i) \\ &+ b_k \bar{b}_m \overline{\boldsymbol{C}}_k(i)\boldsymbol{C}_m(i)\boldsymbol{C}_j(i) \\ &+ \bar{b}_k b_m \boldsymbol{C}_k(i)\overline{\boldsymbol{C}}_m(i)\boldsymbol{C}_j(i) \\ &+ \bar{b}_k \bar{b}_m \boldsymbol{C}_k(i)\boldsymbol{C}_m(i)\boldsymbol{C}_j(i)] \end{aligned} \,. \tag{14c}$$

$$\left\langle \boldsymbol{I}_4^2 \right\rangle = \frac{B\Re^2 P_{sr}^2}{2N\Delta\nu} \sum_{i=1}^{N} \sum_{k=1}^{K} \sum_{m=1}^{K} [b_k b_m \overline{\boldsymbol{C}}_k(i)\overline{\boldsymbol{C}}_m(i)\overline{\boldsymbol{C}}_j(i) + b_k \overline{b}_m \overline{\boldsymbol{C}}_k(i)\boldsymbol{C}_m(i)\overline{\boldsymbol{C}}_j(i) + \overline{b}_k b_m \boldsymbol{C}_k(i)\overline{\boldsymbol{C}}_m(i)\overline{\boldsymbol{C}}_j(i) + \overline{b}_k \overline{b}_m \boldsymbol{C}_k(i)\boldsymbol{C}_m(i)\overline{\boldsymbol{C}}_j(i)] \quad . \tag{14d}$$

The total variance of the photocurrent resulting from the PIIN involves all four PDs would be gotten. Performing the summation of (14a) to (14d), the total variance of the photocurrent would be gotten.

$$\left\langle \boldsymbol{I}_{\text{PIIN}}^2 \right\rangle = \left\langle \boldsymbol{I}_1^2 \right\rangle + \left\langle \boldsymbol{I}_2^2 \right\rangle + \left\langle \boldsymbol{I}_3^2 \right\rangle + \left\langle \boldsymbol{I}_4^2 \right\rangle . \tag{15}$$

Depending on the relation of $\sum_{i=1}^{N} \boldsymbol{C}_j(i) + \overline{\boldsymbol{C}}_j(i) = N$, and the statement of [20],Equ. (15) could be represented as

$$\begin{aligned} \left\langle \boldsymbol{I}_{\text{PIIN}}^2 \right\rangle &= \frac{B\Re^2 P_{sr}^2}{2N\Delta\nu} [\frac{N}{2} K + \alpha \frac{N}{4} K(K-1)] \times 2 \\ &= \frac{B\Re^2 P_{sr}^2}{4\Delta\nu} (\alpha K^2 - \alpha K + 2K) \end{aligned} \quad . \tag{16}$$

where α denotes the polarization-match factor. It means the SOPs mutually match extent between the encoder and decoder. Depending on [20], if the polarization matches when a differential-detection technique is used, the PIIN can be degraded effectively. So, the cross collision may be eliminated completely in perfect condition.

In addition, the DOP must be considered under real condition. Thus, (16) must be multiplied $(1+P^2)$ then becomes the last result to represent total PIIN in our system.

$$(1+P^2)\left\langle \boldsymbol{I}_{\text{PIIN}}^2 \right\rangle = \frac{B\Re^2 P_{sr}^2}{2\Delta\nu} (\alpha K^2 - \alpha K + 2K) . \tag{17}$$

4.3 Signal to PIIN Ratio Evaluation

However, on the long-haul transmissions over OCDMA network the DOP effect must be addressed. In the following analyses, we assume an average value, i.e., α is 1/2. Dividing (10) by (17), the SNR due to the effect of PIIN is

$$\text{SNR}_{(\text{PIIN})} = \frac{\left\langle \boldsymbol{I}_{b=1} - \boldsymbol{I}_{b=0} \right\rangle^2}{\left\langle \boldsymbol{I}_{\text{PIIN}}^2 \right\rangle} = \frac{8\Delta\nu}{BK(K+3)} . \tag{18}$$

The relation between SNR and simultaneous active users of conventional unipolar, bipolar, previous SPC scheme over FBG-base [10], and we propose SPC with polarization-division balanced detector embedded OCDMA system as shown in Table 2. Table 2 presents the character comparison for four kinds of techniques base on Walsh-Hadamard code and only PIIN is considered. The $\text{SNR}_{(\text{PIIN})}$ of proposed

Table 2. Comparisons of different coding schemes with differential-detector over OCDMA network

Adopted scheme	Code length	User capacity	$SNR_{(PIIN)}$
Unipolar SAC	N	N-1	$\frac{\Delta v}{BK(K+1)}$
Bipolar SAC	N	N-1	$\frac{4\Delta v}{BK(K+1)}$
Previous SPC	N	N	$\frac{8\Delta v}{BK(K+1)}$
Proposed SPC with polarization division detector	N	N	$\frac{8\Delta v}{BK(K+3)}$

SPC with double balanced detector structure would be 9 and 3 dB improvement than the conventional unipolar and bipolar SAC schemes, respectively. However, it would be a little worse than the previous SPC scheme when a compromising position is considered. This is because of our design without using any depolarizer. If the polarization match extent is improved, our system will obtain better performance even than hybrid SPC-SAC scheme [22].

Further, the SNR result is substituting into the following Eq. by using the Gaussian assumption as following

$$\mathrm{BER} = \frac{1}{2}\mathrm{erfc}[(\frac{\mathrm{SNR}_{(\mathrm{PIIN})}}{8})^{\frac{1}{2}}]. \tag{19}$$

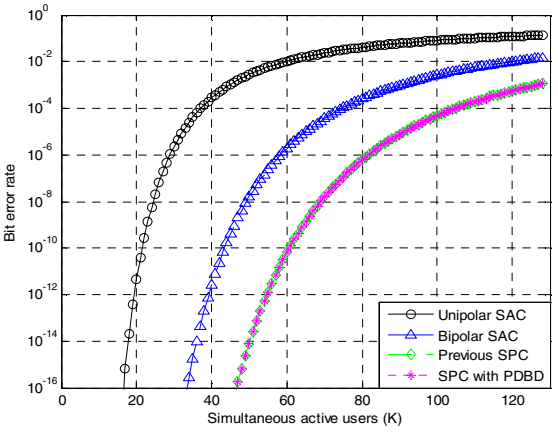

Fig. 3. BER vs. the number of simultaneous active users for different encoding schemes with Walsh-Hadamard code

The relationship between BER and the number of active users for various Hadamard-coded SAC and SPC schemes of OCDMA system is as shown in Fig. 3 based on (19). Transmitting the data bits on two mutually orthogonal SOPs causes some of the PIIN terms to be canceled out. The evaluation results have shown that the use of orthogonal polarizations improves BER. The following parameters: $\Delta\nu = 6.25$ THz, $B = 80$ MHz, and the center wavelength is working at 1550 nm are used in our analysis.

5 Simulations and Discussions

If we think about the shot noise and thermal noise into total noise power for real noise condition, and (17) is substituted for the middle term of (11). Then (11) is adopted as the variance of photocurrent of noise and rewritten as

$$\begin{aligned}\left\langle i^2 \right\rangle &= \left\langle \boldsymbol{I}_{\text{shot}}^2 \right\rangle + \left\langle \boldsymbol{I}_{\text{PIIN}}^2 \right\rangle + \left\langle \boldsymbol{I}_{\text{thermal}}^2 \right\rangle \\ &= 2e\boldsymbol{I}\,B + \boldsymbol{I}^2 B\tau_c + 4K_bT_nB/R_L \\ &= 2e\frac{\Re P_{sr}}{\sqrt{2}}B + \frac{B\Re^2P_{sr}^2}{4\Delta\nu}K(K+3) + \frac{4K_bT_nB}{R_L}\end{aligned} \quad . \tag{20}$$

Using the result of (20), the SNR which is involved the shot noise, PIIN, and thermal noise could be represented as

$$\text{SNR}_{(\text{total})} = \frac{2\Re^2P_{sr}^2}{2e\Re P_{sr}B/\sqrt{2} + B\Re^2P_{sr}^2K(K+3)/4\Delta\nu + 4K_bT_nB/R_L} . \tag{21}$$

Hence, we can draw the related curve of the BER and the effective received power under the different number of simultaneous active user, i.e., $K = 55$, 63, and 71, for we proposed system, as shown in Fig. 4. Clearly, when the effective power is smaller than 10^{-7}w, the proposed system appears high BER. When the received effective power is increased, the BER has apparent improvement. After the effective power is greater than 1μw, even if we continue to increase the power level, the BER keeps in constant value.

Following, the same related curve would be shown under the different coding schemes as shown in Fig. 5. We compare the proposed SPC with unipolar and bipolar SACs, previous SPC with $P = 0$ and 1 under the number of simultaneous active user equals 63. In the plenty simultaneous active user situation, the performance of conventional unipolar coding scheme is awful. The bipolar SAC and SPC with $P = 1$ schemes have approach BER. The BER of the system we proposed is slightly worse than SPC with $P = 0$. However, this scheme does not request the DOP equals 1, namely we do not scatter the polarization state in our system. As long as the effective power achieves certain level, the performances of two schemes will be the same.

In (16), we introduce a polarization-match factor to indicate the SOPs mutually match extent between the encoder and the decoder. Above analyses, we take a compromising condition into account and order $\alpha = 1/2$. Certainly, when the polarization states of the system are matched perfectly, the PIIN from cross collision among different wavelengths will be eliminated completely because of α becomes

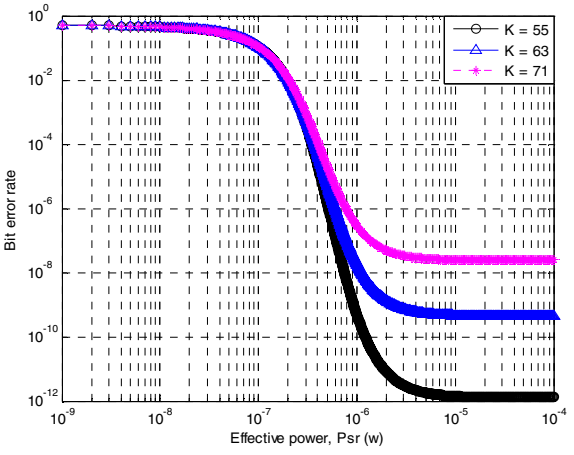

Fig. 4. BER vs. effective power with α = 0.5 and considering total noise for different number of simultaneous active user

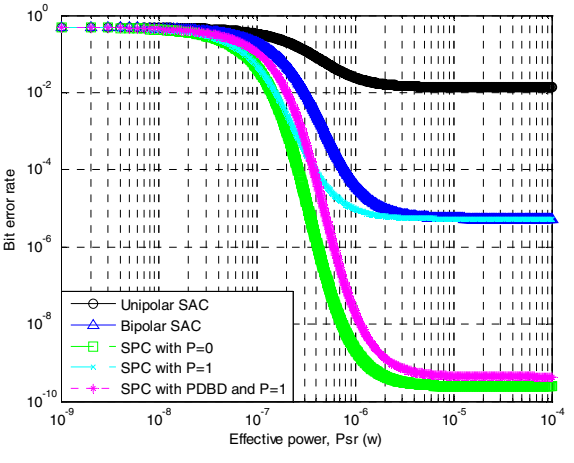

Fig. 5. BER vs. effective power with α = 0.5 and considering total noise for different encoding schemes under 63 simultaneous active user

zero. On the other hand, the PIIN is maximum for the proposed mechanism while α equals 1. Figure 6 discusses four different conditions of α to realize them how to affect the performance of the system. Then the BER analysis and comparison under previous SPC, hybrid SPC-SAC, and proposed SPC with three different polarization-match factors is shown in Fig. 7. According to the simulated result, when α achieves 0.25, the performance of our proposed system is near hybrid SPC-SAC scheme.

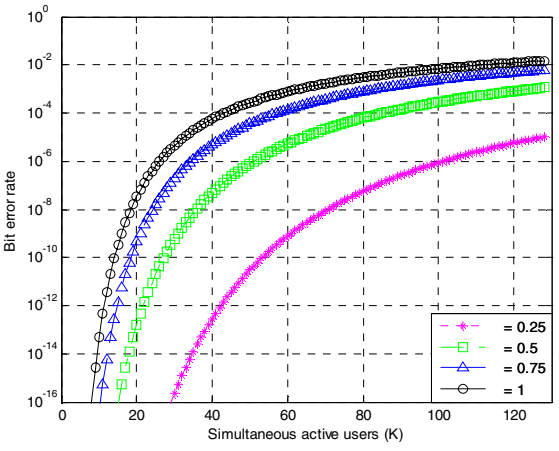

Fig. 6. BER analysis of the proposed system for four different polarization-match factors, i.e., $\alpha = 0.25, 0.5, 0.75$, and 1

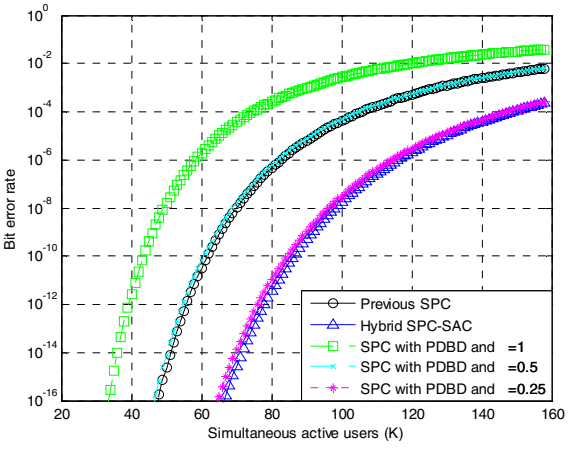

Fig. 7. Performance comparison between the proposed system with three different α and previous SPC scheme

6 Conclusions

In this study, we proposed the modified SPC-OCDMA system structure constructed of hybrid AWG routers and PBSs were implemented over differential photo-detectors. This scheme not only cancels completely the effect of the MAI but also suppresses the PIIN in the multiuser system when the SOPs are controlled. The BER of the OCDMA system has been analyzed numerically for the PIIN limited case. Transmitting the data bits of two users from one encoder on mutually orthogonal SOPs causes some of the PIIN terms to be canceled out. The evaluation results have shown that the use of orthogonal polarizations improves the SNR. However, as the number of active users

increase, the number of PIIN terms which vanish is reduced relative to the total number of incoherent beating terms and hence the noise suppression effect is diminished. The SNR of proposed SPC with polarization-division double balanced detection structure setting DOP to 1 (i.e., $P = 1$) would be found 9 and 3 dB better than the conventional unipolar and bipolar SAC schemes when the DOP is set to zero, respectively. And if the polarization of the system could be matched enough, the performance will achieve the same level with hybrid SPC-SAC scheme.

References

[1] Salehi, J.A.: Code division multiple-access techniques in optical fiber network-Part I: Fundamental principles. IEEE Trans. Commun. 37, 824–833 (1989)

[2] Salehi, J.A., Brackett, C.A.: Code division multiple-access Techniques in optical fiber networks-Part II: Systems performance analysis. IEEE Trans. Commun. 37, 834–842 (1989)

[3] Wei, Z., Shalaby, H.M.H., Ghafouri-Shiraz, H.: Modified quadratic congruence codes for fiber bragg-grating-based spectral-amplitude-coding optical CDMA systems. J. Lightwave Technol. 19, 1274–1281 (2001)

[4] Zhou, X., Shalaby, H.M.H., Lu, C., Cheng, T.: Code for spectral amplitude coding optical CDMA systems. Electron. Lett. 36, 728–729 (2000)

[5] Huang, J.F., Yang, C.C.: Reductions of multiple-access interference in fiber-grating-based optical CDMA network. IEEE Trans. Commun. 50, 1680–1687 (2002)

[6] Moslehi, B.: Noise power spectra of optical two-beam interferometers induced by the laser phase noise. J. Lightwave Technol. 4, 1704–1710 (1986)

[7] Smith, E.D.J., Baikie, R.J., Taylor, D.P.: Performance enhancement of spectral-amplitude-coding optical CDMA using pulseposition modulation. IEEE Trans. Commun. 46, 1176–1185 (1998)

[8] Smith, E.D.J., Gough, P.T., Taylor, D.P.: Noise limits of optical spectral-encoding CDMA systems. Electron. Lett. 31, 1469–1470 (1995)

[9] Huang, J.F., Yang, C.C., Tseng, S.P.: Complementary Walsh-Hadamard coded optical CDMA coder/decoders structured over arrayed-waveguide grating routers. Optics Commun. 229, 241–248 (2004)

[10] Chang, Y.T., Huang, J.F.: Complementary bipolar spectral polarization coding over fiber-grating-based differential photodetectors. Optical Engineering 45, 045004 (2006)

[11] Hu, H.W., Chen, H.T., Yang, G.C., Kwong, W.C.: Synchronous walsh-based bipolar-bipolar code for CDMA passive optical networks. J. Lightwave Technol. 25, 1910–1917 (2007)

[12] Sekine, K., Sasaki, S., Kikuchi, N.: 10 Gbit/s four-channel wavelength- and polarisation-division multiplexing transmission over 340 km with 0.5 nm channel spacing. Electron. Lett. 31, 49–50 (1995)

[13] Sotobayashi, H., Chujo, W., Kitayama, K.: 1.6-b/s/Hz 6.4-Tb/s QPSK-OCDM/WDM (4 OCDM × 40 WDM × 40 Gb/s) transmission experiment using optical hard thresholding. IEEE Photon. Technol. Lett. 14, 555–557 (2002)

[14] Tsalamanis, I., Rochat, E., Walker, S., Parker, M., Holburn, D.: Experimental demonstration of cascaded AWG access network featuring bi-directional transmission and polarization multiplexing. Opt. Express 12, 764–769 (2004)

[15] Chraplyvy, A.R., Gnauck, A.H., Tkach, R.W., Zyskind, J.L., Sulhoff, J.W., Lucero, A.J., Sun, Y., Jopson, R.M., Forghieri, F., Derosier, R.M., Wolf, C., McConnick, A.R.: 1-Tb/s Transmission Experiment. IEEE Photonics Technol. Lett. 13, 1370–1372 (2001)

[16] Poole, C.D., Wagner, R.E.: Phenomenological approach to polarization dispersion in long single-mode fibres. Electron. Lett. 22, 1029–1030 (1986)

[17] Khosravni, R., Havstad, S.A., Song, Y.W., Ebrahimi, P., Willner, A.E.: Polarization-mode dispersion compensation in WDM systems. IEEE Photonics Technol. Lett. 13, 1370–1372 (2001)

[18] Willner, A.E., Motaghian Nezam, S.M.R., Yan, L., Pan, Z., Hauer, M.C.: Monitoring and control of polarization-related impairments in optical fiber systems. J. Lightwave Technol. 22, 106–125 (2004)

[19] Heismann, F., Hansen, P.B., Korotky, S.K., Raybon, G., Veselka, J.J., Whalen, M.S.: Automatic polarisation demultiplexer for polarisation-multiplexedtransmission systems. Electron. Lett. 29, 1965–1966 (1986)

[20] Chan, E.H.W., Minasian, R.A.: Suppression of phase-induced intensity noise in optical delay-line signal processors using a differential-detection technique. IEEE Trans. Microw. Theory Tech. 54, 873–879 (2006)

[21] Poole, C.D., Bergano, N.S., Wagner, R.E., Schulte, H.J.: Polarization dispersion and principal states in a 147-km undersea lightwave cable. J. Lightwave Technol. 6, 1185–1190 (1988)

[22] Huang, J.F., Chang, Y.T.: Improved phase noise performance using orthogonal ternary codes over spectral polarization and amplitude coding networks. Opt. Eng. 46, 015005 (2007)